Abstract

Many aquifers around the world are impacted by toxic chlorinated methanes derived from industrial processes due to accidental spills. Frequently, these contaminants co-occur with chlorinated ethenes and/or chlorinated benzenes in groundwater, forming complex mixtures that become very difficult to remediate. In this study, a multi-method approach was used to provide lines of evidence of natural attenuation processes and potential setbacks in the implementation of bioremediation strategies in multi-contaminated aquifers. First, this study determined i) the carbon and chlorine isotopic compositions ($\delta^{13}C$, $\delta^{37}Cl$) of several commercial pure phase chlorinated compounds, and ii) the chlorine isotopic fractionation ($\varepsilon Cl = -5.2 \pm 0.6‰$) and the dual C–Cl isotope correlation ($\Lambda^{C/Cl} = 5.9 \pm 0.3$) during dichloromethane (DCM) degradation by a *Dehalobacterium*-containing culture. Such data provide valuable information for practitioners to support the interpretation of stable isotope analyses derived from polluted sites. Second, the bioremediation potential of two industrial sites contaminated with a mixture of organic pollutants (mainly DCM, chloroform (CF), trichloroethene (TCE), and mono-chlorobenzene (MCB)) was evaluated. Hydrochemistry, dual (C–Cl) isotope analyses, laboratory microcosms, and microbiological data were used to investigate the origin, fate and biodegradation potential of chlorinated methanes. At Site 1, $\delta^{13}C$ and $\delta^{37}Cl$ compositions from field samples were consistent with laboratory microcosms, which showed complete degradation of CF, DCM and TCE, while MCB remained. Identification of *Dehalobacter* sp. in CF-enriched microcosms further supported the biodegradation capability of the aquifer to remediate chlorinated methanes. At Site 2, hydrochemistry and $\delta^{13}C$ and $\delta^{37}Cl$ compositions from field samples suggested little DCM, CF and TCE transformation; however, laboratory microcosms evidenced that their degradation was severely inhibited, probably by co-contamination. A dual C-Cl isotopic

assessment using results from this study and reference values from the literature allowed to determine the extent of degradation and elucidated the origin of chlorinated methanes.

1. Introduction

Dichloromethane (DCM) is a probable human carcinogen (IARC, 2016), included in the list of priority pollutants of both the U.S. Agency for Toxic Substances and Disease Registry (2016) and the European Commission (2012). DCM can be naturally released by oceanic sources, wetlands, volcanoes and macroalgae (Gribble, 2010), but its detection in groundwater is often a result of its extensive use, accidental spills and improper storage in chemical, pharmaceutical, and petroleum industrial facilities, among others (Marshall and Pottenger, 2016).

Numerous bacteria capable of using DCM as a growth substrate under aerobic conditions have been identified, including various strains of *Hyphomicrobium* (Heraty et al., 1999; Hermon et al., 2018; Nikolausz et al., 2006) and *Methylobacterium* (Torgonskaya et al., 2019). The aerobic pathway for DCM biodegradation begins with a glutathione S-transferase producing formaldehyde, which is partially oxidized to CO_2 and chloride (Muller et al., 2011). To date, anaerobic biodegradation of DCM has been solely reported for bacteria affiliated with the *Peptococcaceae* family: *Dehalobacterium*, *Dehalobacter*, and *Candidatus* Dichloromethanomonas elyunquensis (D. elyunquensis). *Dehalobacterium formicoaceticum* (*Dhb f.*) is the only pure culture described using DCM as carbon and energy source under anoxic conditions, and produces formate and acetate as end products (Mägli et al., 1998). Recently, mixed bacterial cultures containing *Dehalobacter* sp. and/or D. elyunquensis have been reported to ferment DCM to mainly acetate (Chen et al., 2017; Justicia-Leon et al., 2012; Kleindienst et al., 2017; Lee et al., 2015, 2012).

Besides direct release into groundwater, DCM can also be produced by dehalogenation of the higher chlorinated methanes (CMs), i.e. carbon tetrachloride (CT) or chloroform (CF). The latter is listed as a probable carcinogen and a priority

contaminant as well (ATSDR, 2016; European Commission, 2012; IARC, 2018). Under anoxic conditions, DCM might derive either from the hydrogenolysis of CF by the organohalide-respiring bacteria *Dehalobacter* sp. and *Desulfitobacterium* sp. (Chan et al., 2012; Ding et al., 2014; Tang and Edwards, 2013; Wong et al., 2016). Also, the anaerobic degradation of CF by *Acetobacterium* sp. comprises both a reductive branch leading to DCM and an oxidative pathway leading to CO_2 (Egli et al., 1990, 1988; Wanner et al., 2018). DCM can be also produced co-metabolically by, for example, *Methanosarcina* sp. or *Clostridium* sp. (Egli et al., 1988; Gälli and McCarty, 1989; Krone et al., 1989b, 1989a; Mikesell and Boyd, 1990).

Chlorinated solvents are commonly found in complex mixtures in groundwater from contaminated sites rather than as individual chemicals. In multi-contaminated aquifers, microbial degradation can be affected and even inhibited by co-contaminants. This information is relevant to foresee the efficiency of natural attenuation or enhanced bioremediation strategies. For instance, the inhibitory effects of CF on key microbial processes such as methanogenesis and microbial dechlorination reactions of chlorinated ethenes (CEs) and ethanes are well known (Weathers and Parkin, 2000; Wei et al., 2016). In addition, it has also been reported that CT and CF inhibit their mutual biodegradation (da Lima and Sleep, 2010; Grostern et al., 2010; Justicia-Leon et al., 2014).

Compound-specific isotope analysis (CSIA) is a useful tool that allows bioremediation practitioners to assess the effectiveness of remediation treatments. During chemical or biological degradation of target contaminants, bonds containing the lighter isotopes are preferentially broken, causing the remaining contaminant to be enriched in the heavier isotopes compared to the original isotopic value (Aelion et al., 2009). This is quantified through the abundance ratio of specific stable isotopes (e.g. $^{13}C/^{12}C$, $^{37}Cl/^{35}Cl$) in contaminant molecules relative to an international standard (Aelion et al., 2009). This

technique may be used for source apportionment as well as the monitoring of transformation processes in the field (Elsner, 2010). In addition, a quantitative estimation of contaminant transformation extent in the field can be possible, provided that the isotope fractionation (ε) for a given compound and degradation pathway are known and well constrained (Aelion et al., 2009).

Dual element isotope analysis has some advantages over a single element isotope approach. On the one hand, by improving the identification of the source (either related to commercial solvents release or from parent compound degradation); on the other, by allowing the elucidation of the fate of pollutants in the field. During biodegradation processes, single element intrinsic isotope effects related to C–Cl bond cleavage can be masked due to the occurrence of previous rate-limiting steps such as preceding enzymatic reactions (Sherwood Lollar et al., 2010), bioavailability of electron donor and/or acceptor (Aeppli et al., 2009; Kampara et al., 2008; Thullner et al., 2008), substrate uptake and transport through the cell membrane (Cichocka et al., 2007; Renpenning et al., 2015), among others. These processes are generally non- or slightly-isotope fractionating so that both elements (e.g. C and Cl) are affected similarly. In this case, by taking the ratio of the isotope shift for the two elements (e.g. $\Lambda = \Delta\delta^{13}C / \Delta\delta^{37}Cl$), their masking effect is cancelled out and these slopes reflect better the ongoing degradation mechanisms (Elsner, 2010). While single element isotope fractionation could provide insight into the underlying reaction mechanisms in laboratory biodegradation experiments, this is not possible under field conditions. The reason is that contaminant concentration changes at the field are also related to processes other than its transformation (such as sorption and hydrodynamic dispersion), preventing accurate calculation of ε values. Thus, Λ values determined from laboratory studied reactions can be compared with those obtained from groundwater samples to investigate degradation processes at the field scale (Badin et al.,

2014; Hermon et al., 2018; Hunkeler et al., 2009; Palau et al., 2017; Rodríguez-Fernández et al., 2018b).

Several laboratory studies have applied dual C–Cl isotope analysis to describe biotic and abiotic transformation mechanisms for DCM (Chen et al., 2018; Heraty et al., 1999; Torgonskaya et al., 2019) and CF (Heckel et al., 2019, 2017a; Rodríguez-Fernández et al., 2018a; Torrentó et al., 2017) but, to the best of the author's knowledge, the application of a dual isotope approach in DCM-contaminated sites has not been reported yet.

The purpose of the work presented herein is two-fold. First, it aims to determine i) the $\Lambda^{C/Cl}$ value for the anaerobic degradation of DCM by a *Dehalobacterium*-containing culture, and ii) the carbon and chlorine isotopic compositions ($\delta^{13}C$, $\delta^{37}Cl$) of several commercial pure phase DCM and CF. These new isotope data enrich the database to which dual C–Cl isotopes slopes measured in the field can be compared to elucidate degradation mechanisms. Second, a multi-method approach was used at two industrial sites impacted by DCM, CF, trichloroethene (TCE) and mono-chlorobenzene (MCB) to investigate their origin, fate and intrinsic biodegradation potential. To this end, hydrochemical conditions in groundwater, concentrations of target contaminants and their stable isotope ratios ($\delta^{13}C$, $\delta^{37}Cl$) in field samples were analysed. Afterwards, a dual C–Cl isotopic assessment using the results from this study and reference values from the literature was performed to reveal the origin and fate of DCM. Lastly, field-derived microcosms testing for biostimulation as well as bioaugmentation, and 16S rRNA high-throughput sequencing were performed to assess the intrinsic biodegradation potential of target contaminants at the sites.

2. Materials and methods

131 *2.1. Materials*

132 Pure phase chlorinated compounds isotopically characterised and/or used for the
133 experiments were purchased at the highest purity available from the following suppliers:
134 CF (Sigma Aldrich, Alfa, Merck), DCM (Sigma Aldrich, Fisher, SDS, Merck), MCB
135 (Sigma Aldrich) and TCE (Panreac). CF (Sigma Aldrich) was used for the enrichment of
136 field-derived cultures. Industrial grade sodium L-lactate (97% purity, at 60% w/w) was
137 from Purac (Corbion). All other chemicals and reagents used were of the highest purity
138 available.

139 Samples of the time-course degradation of DCM in a culture containing
140 *Dehalobacterium* (*Dhb*) were obtained from a previous study reported elsewhere
141 (Trueba-Santiso et al., 2017).

142 Two different commercial bacterial consortia were used for the microcosm
143 bioaugmentation tests. Detailed information about the products cannot be disclosed due
144 to commercial confidentiality reasons. Commercial inoculum "S" was reported to
145 degrade CF to DCM, and fully dechlorinated CEs to ethene (ETH). Commercial inoculum
146 "M" was reported to degrade CF to methane via DCM and chloromethane.

147 *2.2. Hydrogeochemistry of the studied sites*

148 The sites are located in the Catalan Coastal Ranges, which are characterized by an
149 echelon fault system, subparallel to the coast, that affected the Hercynian basement and
150 the Mesozoic overlying sediments. The Neogene extension created a "horst and graben"
151 system filled by Miocene and Quaternary sediments. Both sites are located in the Neogene
152 basin, one of them in the Miocene sediments and the other in the granitic basement.

153 **Site 1**

154 The studied site is located at an industrial area in the Barcelona province (Spain).
155 Geologically, it is constituted by clays and conglomerates of quaternary age overlying
156 unconformable upper Miocene siliciclastic sediments that dip 15–20º in the NW
157 direction. Petrologically, the Miocene sediments are represented by clay and sands
158 composed of abundant quartz grains, mica and kaolinized feldspars and, locally, by some
159 conglomerates. Hydrogeologically, Miocene aquifer has an average transmissivity of 5–
160 180 m^2/d, less than the alluvial aquifer. A geological cross section of the studied area can
161 be found in Section A of the Supporting Information (SI).

162 A previous characterization of the site detected high loads of contaminants and dense
163 nonaqueous phase liquid (DNAPL) in groundwater, which was originated after improper
164 storage of the substances (Figure 1A, SI section A). The main organic halogenated
165 compounds included DCM, CF, TCE, and MCB, but *cis*-1,2-dichloroethene (*cis*-DCE),
166 vinyl chloride (VC), tetrachloroethene (PCE), acetone, BTEX, and tetrahydrofuran were
167 also detected. The contamination plume was considered finite and contained. After the
168 initial site characterization, a pump and treat (P&T) remediation system (groundwater
169 extraction) was implemented. Under this ongoing treatment, groundwater flowed radially
170 towards the extraction points and a total of seven conventional fully screened monitoring
171 wells were sampled (Figure 1A, SI section B).

172 **Site 2**

173 This site is also located at an industrial zone in the Barcelona province (Spain), but
174 more than 30 km apart from Site 1. Geologically, it is constituted by Quaternary alluvial
175 sediments represented by sands and gravels that overlie unconformably the basement of
176 the Neogen basin made by later-Hercynian intrusive granites. Hydrogeologically,
177 groundwater flows mainly from the alluvial gravels to the river freshwater and, to a lesser
178 extent, through the more fractured and weathered granite. A conceptual site model of the

179 studied area can be found in SI section C.

180 Like in Site 1, it was previously confirmed that the aquifer in Site 2, originally
181 contaminated because of improper management, contained DNAPL (Figure 2A, SI
182 section C). The most abundant contaminants in groundwater included DCM, CF, TCE,
183 and MCB, but acetone, toluene, PCE, CT, VC, tetrahydrofuran and benzene were also
184 detected in groundwater. After the initial site characterization, dual-phase extraction
185 (DPE) and P&T remediation systems were implemented and ongoing during this study.
186 For the hydrochemical characterization, nine conventional fully screened monitoring
187 wells were sampled (Figure 2A, SI section D). At that time, the groundwater flow
188 direction was E–W, and radially towards the extraction points due to DPE and P&T, and
189 the contamination source was reported to be still active (SI section D).

190 *2.3. Collection of groundwater samples*

191 Hydrochemical parameters (Eh, pH, T and electric conductivity) were measured *in-*
192 *situ* and groundwater samples from selected monitoring wells (see SI sections B and D)
193 were collected as described elsewhere (Blázquez-Pallí et al., 2019). It has to be taken into
194 account that these values are an average of the screen length. Samples for chemical and
195 isotopic analysis were collected in different sampling containers on July 11th and 12th,
196 2017, from Site 1 and Site 2. Groundwater was collected with a peristaltic pump or bailer,
197 depending on the water table depth. Samples for C–Cl CSIA were preserved with HNO_3
198 (pH~2) (Badin et al., 2016) to prevent biodegradation processes. For the microcosm
199 experiments, groundwater with fine sediments from PZ-9, PZ-19 and PZ-36 from Site 2
200 (SI section D) and PI-2 from Site 1 (SI section B) was sampled on the 18th and 19th of
201 June 2018, respectively. All samples were collected in amber glass bottles sealed with
202 PTFE caps and stored in the dark at 4ºC until used.

203 *2.4. Set up of laboratory microcosms*

204 The microcosms were prepared within the following two days after sampling. They
205 consisted of 65 mL of sampled groundwater in 100 mL glass serum sterile bottles sealed
206 with Teflon-coated butyl rubber septa as described elsewhere (Blázquez-Pallí et al.,
207 2019). To investigate whether a potential bioremediation treatment would be feasible at
208 the investigated sites, three different experiments were prepared in triplicate: (i) a control
209 containing only groundwater from the site, which tested for monitored natural attenuation
210 (MNA); (ii) groundwater with sodium lactate (~4 mM), which tested for biostimulation;
211 and (iii) groundwater inoculated with the commercial bacterial consortia described above
212 (10^6–10^7 cells/mL) plus sodium lactate (~4 mM), which tested for bioaugmentation. For
213 the samples from wells PZ-19 and PZ-36 (Site 2, SI section D), two different
214 bioaugmentation tests were established, i.e. one with each commercial inoculum, whereas
215 only one bioaugmentation test (using the commercial inoculum "S") was performed with
216 samples from PZ-9 (Site 2, SI section D) and PI-2 (Site 1, SI section B).

217 To identify the bacteria responsible for CF degradation, the dilution-to-extinction
218 method (Löffler et al., 2005) was applied in 12-mL vials containing an anoxic defined
219 medium described elsewhere (Martín-González et al., 2015) and using CF as electron
220 acceptor. After four extinction series, the more diluted vial showing activity against CF
221 was used as inoculum for serum bottle microcosms, which were selected for 16S rRNA
222 analysis after consuming 1 mM CF. The serum bottle microcosms were prepared as
223 described elsewhere (Martín-González et al., 2015).

224 *2.5. DNA extraction and 16S rRNA gene amplicon sequencing*

225 Biomass was harvested from whole serum bottle microcosms in sterile falcon tubes
226 that were centrifuged for 40 min at 7000 × *g* and 10 ºC in an Avanti J-20 centrifuge. The

pellets were resuspended in sterile PBS buffer and, afterwards, DNA was extracted with the Gentra Puregene Yeast/Bact kit (Qiagen) following the instructions of the manufacturer. Extraction and analysis of the DNA of each microcosm was performed separately. The regions V3–V4 of the 16S rRNA genes were amplified with primers S-D-Bact-0341-b-S-17 and S-D-Bact-0785-a-A-21 (Klindworth et al., 2013) with the Illumina MiSeq platform at *Serveis de Genòmica i Bioinformàtica* from *Universitat Autònoma de Barcelona*.

2.6. Analytical methods

The hydrogeochemical parameters of groundwater (temperature, pH, redox potential (Eh) and electric conductivity) were determined *in-situ* using a multiparameter probe 3430 WTW (Weilheim) as described elsewhere (Blázquez-Pallí et al., 2019).

Chlorinated compounds were quantified by analysing 500 µL of headspace samples by gas chromatography (GC) coupled to a flame ionization detector (FID), as described elsewhere (Martín-González et al., 2015). Lactate, acetate and other short-chain fatty acids (VFAs) were monitored by HPLC from 1 mL filtered liquid samples (0.22 µm, Millex), as previously reported (Mortan et al., 2017).

Stable carbon isotope ratios ($\delta^{13}C$) of pure in-house standards were determined with a Flash EA1112 (Carlo-Erba, Milano, Italy) elemental analyser (EA) coupled to a Delta C isotope ratio mass spectrometer (IRMS) through a Conflo III interface (Thermo Finnigan, Bremen, Germany), while the $\delta^{13}C$ values of target chlorinated compounds (DCM, CF, CEs and MCB) in field samples were obtained by CSIA using an Agilent 6890 GC coupled to a Delta Plus IRMS, as described in Blázquez-Pallí et al. (2019). All analyses (standards and experimental samples) had a one standard deviation (1σ) lower than 0.5‰.

Stable chlorine isotope ratios ($\delta^{37}Cl$) were obtained by CSIA at Isotope Tracer

Technologies Inc., Waterloo (ON, Canada). A 6890 GC (Agilent, Santa Clara, CA, U.S.) coupled to a MAT 253 IRMS (Thermo Finnigan, Bremen, Germany) were used. This IRMS, equipped with nine collectors, is a continuous flow IRMS with a dual-inlet (DI) mode option. The DI bellows are used as the monitoring gas reservoir (either CF or DCM) and reference peaks were introduced at the beginning of each analysis run (Shouakar-Stash et al., 2006). For the analysis of chlorine isotope ratios of CF, the two main ion peaks (*m/z* 83 and 85) were used, which correspond to isotopologue pairs that differ by one heavy chlorine isotope ($[^{\mathbf{35}}\mathbf{Cl_2}^{12}C^{1}H]^{+}$ and $[^{\mathbf{37}}\mathbf{Cl}^{\mathbf{35}}\mathbf{Cl}^{12}C^{1}H]^{+}$, respectively) (Breider and Hunkeler, 2014). For DCM, the chlorine isotopic composition was determined from two ion peaks of the molecular group (*m/z* 84 and 86) corresponding to $[^{\mathbf{35}}\mathbf{Cl_2}^{12}C^{1}H_2]^{+}$ and $[^{\mathbf{37}}\mathbf{Cl}^{\mathbf{35}}\mathbf{Cl}^{12}C^{1}H_2]^{+}$, respectively. Similarly to carbon isotopes analysis, the analytes were extracted by headspace solid-phase microextraction, as shown elsewhere (Palau et al., 2017). Samples and standards were diluted at similar concentrations and measured in duplicate. The $\delta^{37}Cl$ values of pure in-house standards were characterized relative to SMOC (Standard Mean Ocean Chloride) by offline IRMS analysis after conversion of DCM to methyl chloride according to Holt et al. (1997). These standards were later used to correct all measurements from samples. Precision (1σ) of the analysis was ≤ 0.2‰ for $\delta^{37}Cl$.

The isotopic compositions of carbon and chlorine are reported in delta notation ($\delta^{h}E$, in ‰), relative to the international standards VPDB (Vienna Pee Dee Belemnite) and SMOC (Coplen, 1996; Kaufmann et al., 1984), respectively (Eq. 1),

$$\delta^{h}E = \left(\frac{R_{sample}}{R_{std}} - 1\right) \qquad (1)$$

where R_{sample} and R_{std} are the isotope ratios (i.e. $^{13}C/^{12}C$, $^{37}Cl/^{35}Cl$) of the sample and the standard of an element E, respectively (Elsner, 2010).

2.7. Calculations for interpretation of isotopic data

A simplified version of the Rayleigh equation in the logarithmic form (Eq. 2) correlates changes in the isotopic composition of an element in a compound (R_t/R_0) with changes in its concentration for a given reaction ($f = C_t/C_0$), which allows to determine the corresponding isotopic fractionation (ε) (Coplen, 2011; Elsner, 2010).

$$\ln\left(\frac{R_t}{R_0}\right) = \varepsilon \cdot \ln(f) \qquad (2)$$

R_t/R_0 can be expressed as $(\delta^h E_t + 1) / (\delta^h E_0 + 1)$ according to $\delta^h E$ definition. For the experiment of DCM degradation by the stable enrichment culture containing *Dhb*, the εCl was obtained from the slope of the linear regression according to Eq. 2. The uncertainty corresponds to the 95% confidence interval (CI).

For a target contaminant, the extent of degradation (D%) in the field was evaluated with Eq. 3, which is derived from the Rayleigh equation (Eq. 2),

$$D\% = \left[1 - \left(\frac{\delta^h E_t + 1000}{\delta^h E_0 + 1000}\right)^{\frac{1000}{\varepsilon E}}\right] \cdot 100 \qquad (3)$$

where εE refers to the isotopic fractionation, $\delta^h E_t$ are the isotope data from groundwater samples and $\delta^h E_0$ is the most depleted value found at the field site, assumed to be the most similar to the original source. To this regard, differences in isotope values in the field for both carbon and chlorine ($\Delta\delta^{13}C$, $\Delta\delta^{37}Cl$) must be >2‰ for degradation to be considered significant (Hunkeler et al., 2008). Laboratory derived ε values can either be site-specific (i.e., from microcosm experiments prepared with soil and/or groundwater from the contaminated site) or obtained from the literature (Table 1).

Finally, the $\Lambda^{C/Cl}$ value for the DCM biodegradation experiment was obtained from the slope of the linear regression in the dual C–Cl isotope plot (Elsner, 2010) and the

297 uncertainty is the 95% CI.

298 *2.8. Dual C–Cl isotopic assessment based on selected $\Lambda^{C/Cl}$*

299 To understand the origin and fate of DCM and CF at each site, a dual C–Cl isotopic
300 assessment (Badin et al., 2016; Hunkeler et al., 2008) was performed based on the
301 measured $\delta^{13}C$ and $\delta^{37}Cl$ data of field and commercial compounds, the definition of D%
302 (Eq. 3), and εC, εCl and $\Lambda^{C/Cl}$ from the available literature (Tables 1 and 2). The procedure
303 followed for the dual C–Cl isotopic assessment is detailed in SI section E.

304

305 **3. Results and discussion**

306 *3.1. $\delta^{13}C$ and $\delta^{37}Cl$ of pure in-house commercial standards*

307 Several pure in-house commercial standards were analysed to determine their $\delta^{13}C$ and
308 $\delta^{37}Cl$ compositions (see details in Table 2). $\delta^{13}C_{DCM}$ for the standards that were measured
309 in this study ranged from -35.4 ± 0.2 to -41.71 ± 0.08‰, while $\delta^{37}Cl_{DCM}$ ranged from +2.1
310 ± 0.3 to -2.7 ± 0.1‰. $\delta^{13}C_{CF}$ ranged from -47.96 ± 0.06 to -52.7 ± 0.1‰, while $\delta^{37}Cl_{CF}$
311 ranged from -2.6 ± 0.1 to -5.9 ± 0.2‰. A significant variation was observed among the
312 different DCM and CF commercial standards analysed in this study, but also when
313 compared to some of the values available in the literature. For instance, the $\delta^{37}Cl_{DCM}$
314 value obtained for the Fisher standard (-2.7 ± 0.1‰) is more depleted in ^{37}Cl than the
315 values available to date (Table 2), emphasizing the relevance of reference isotopic
316 composition of the pure products provided in this study for future data interpretation.
317 Lastly, $\delta^{13}C$ for TCE and MCB was also analysed here and resulted in -25.40 ± 0.03‰
318 and -27.09 ± 0.07‰, respectively.

319 *3.2. Chlorine isotope fractionation and $\Lambda^{C/Cl}$ during anaerobic DCM degradation by a*
320 *Dhb-containing culture*

Samples of a *Dhb*-containing culture that were previously killed to analyse the decrease of concentration and the carbon isotope fractionation of DCM (Trueba-Santiso et al., 2017) were used in this study. The $\delta^{37}Cl$ during DCM degradation increased from -5.7 ± 0.2 to +7.2 ± 0.2‰ after 97% transformation, but neither changes in concentration nor in $\delta^{37}Cl$ (average -5.7 ± 0.2‰) were observed in the abiotic controls. However, this last point (97%) was excluded because it appeared to be deviated from the linear regression (R^2=0.95, Eq. 2), whereas the best-fitting was obtained for $\delta^{37}Cl$ values up to 84% degradation (R^2=0.98) leading to a εCl of -5.2 ± 0.6‰ (Figure 3A). This phenomenon was observed previously by Mundle et al. (2013), who reported higher uncertainty in ε values calculated at later stages of the reaction and suggested examining the linearity of the fits over shorter reaction progress intervals. To date, there is still no εCl value available for *Dehalobacter*, but the εCl value of -5.2 ± 0.6‰ obtained in this study for *Dhb* is not significantly different from those reported for D. elyunquensis (-5.2 ± 0.1‰), *Dhb f.* (-5.3 ± 0.1‰), and purified dehalogenases of *M. extorquens* DM4 and *Methylophilus leisingeri* DM11(-5.7 and -5.6‰, respectively) (Chen et al., 2018; Torgonskaya et al., 2019) according to the student's *t*-test (8 degrees of freedom, p=0.05). In contrast, it is significantly different than those reported for *Hyphomicrobium* sp. strain MC8b (-3.8‰) and *Methylobacterium extorquens* DM4 (-7.0‰) (Heraty et al., 1999; Torgonskaya et al., 2019) (Table 1).

The εC recalculated up to 84% degradation for *Dhb* (-31 ± 3‰, R^2=0.986) does not vary much from the previously published value (-27 ± 2‰, R^2=0.985) (Trueba-Santiso et al., 2017), and still differ from the reported DCM-fermentative bacteria *Dehalobacter* (-16 ± 2‰) (Lee et al., 2015). However, recent studies on *Hyphomicrobium* sp. strains (Hermon et al., 2018) and *Methylobacterium extorquens* DM4 (Torgonskaya et al., 2019) has widened the εC range attributed to methylotrophic bacteria (-22 to -66.6‰), not

allowing to distinguish hydrolytic transformation of DCM via glutathione-dependent dehalogenases and fermentation pathway just by carbon isotopes.

A very good linear correlation (R^2=0.995) was also obtained for $\delta^{13}C$ against $\delta^{37}Cl$ values up to 84% degradation in a dual C–Cl isotope plot ($\Lambda^{C/Cl}$ of 5.9 ± 0.3, Figure 3B). This $\Lambda^{C/Cl}$ value by the *Dhb*-containing culture is significantly different from those reported for D. elyunquensis ($\Lambda^{C/Cl}$ = 3.40 ± 0.03) and for *Dhb f.* ($\Lambda^{C/Cl}$ = 7.89 ± 0.12) (Chen et al., 2018) (Figure 3B) according to the student's *t* test (8 degrees of freedom, p=0.05). The difference between *Dhb* and D. elyunquensis is in accordance with recent proteogenomic findings suggesting that both genera have distinct DCM degradation pathways (Kleindienst et al., 2019). However, the difference observed between *Dhb* and *Dhb f.* may suggest that they either have mechanistic disparities during DCM degradation, even though they both belong to the same genus. Higher $\Lambda^{C/Cl}$ values, ranging from 8.1 to 11.2, have been reported for the aerobic *Hyphomicrobium* sp. strain MC8b (Heraty et al., 1999), *Methylobacterium extorquens* DM4, and DM4 and DM11 DCM dehalogenases (Torgonskaya et al., 2019). To date, these values hint at the distinction between aerobic (11.2 to 8.1) and anaerobic (7.89 to 3.40) pathways (Figure 3B). However, further research on this topic would be needed to confirm such hypothesis. See Table 1 for a detailed review of literature values.

3.3. Field sites investigation

3.3.1. Site 1

The studied aquifer exhibited mixed redox conditions (Eh ranged from +250 to -52) mV), but most of the wells were in anoxic conditions (SI section F), which are conducive

370 to reductive dechlorination reactions. Temperature and pH were considered homogeneous
371 throughout the aquifer (21.1 ± 0.7 ºC and 6.8 ± 0.3, respectively) (SI section F). CF was
372 the organohalide detected at the highest concentration (454 mg/L), followed by MCB
373 (82.7 mg/L), TCE (47.2 mg/L), and DCM (1.47 mg/L) (Figure 1A and SI section G).

374 The C–Cl isotopic composition of CF could be determined in 5 out of 7 monitoring
375 wells (Figure 1A). Obtained $\delta^{13}C$ values for CF showed a relatively small but significant
376 variation ($\Delta\delta^{13}C_{CF}$) of 3.2‰ between wells PI-17 and CV-5, which exhibited the most
377 enriched and depleted $\delta^{13}C_{CF}$, respectively (SI section H). Since the difference in the
378 carbon isotope composition was >2‰, it could be related to CF transformation in
379 groundwater (Hunkeler et al., 2008). In contrast, the maximum $\Delta\delta^{37}Cl_{CF}$ observed at the
380 site between wells CV-5 and PI-24 was lower than 2‰. This agrees well with previous
381 studies showing εC values usually greater than εCl during CF biodegradation (Table 1).
382 The dual isotopic composition of CF in the analysed groundwater samples fell outside the
383 isotopic range of commercial CF, except for samples collected in well CV-5 (SI section
384 I). This result would further support a potential transformation of CF at the site.

385 For DCM, only one C–Cl isotopic composition could be determined (in well PI-26)
386 due to DCM concentration being too low for carbon CSIA, but $\delta^{37}Cl$ could be determined
387 in 4 out of 7 wells (Figure 1A). Obtained $\delta^{37}Cl$ for DCM showed a significant variation
388 in $^{37}Cl/^{35}Cl$ ratios of $\Delta\delta^{37}Cl_{DCM}$ = 2.3‰ between wells CV-5 and PI-26 (SI section H,
389 Figure 1A), and these $\delta^{37}Cl$ were enriched compared to those of commercial DCM (Table
390 2). As mentioned earlier, no $\Delta\delta^{13}C_{DCM}$ can be provided for $\delta^{13}C$ since only one value
391 could be obtained, but this value was also enriched compared to most of the $\delta^{13}C$ reported
392 for commercial DCM (Table 2). Hence, this dual C–Cl isotopic composition for DCM in
393 the analysed groundwater of well PI-26 fell outside the isotopic range of commercial
394 DCM, suggesting a potential transformation of DCM at the site as well (SI section I).

When comparing these results to the literature, the low carbon enrichment observed could indicate that the bacteria responsible for DCM degradation have a εC that is in the lower range (e.g. *Dehalobacter* sp., which has the lowest reported εC as presented in Table 1). An additional evidence pointing towards *in-situ* DCM biodegradation was the detection of acetate in wells PI-26 and CV-3 (Figure 1A and SI section G), which is the main by-product of DCM fermentation (Justicia-Leon et al., 2012; Lee et al., 2015; Mägli et al., 1998; Trueba-Santiso et al., 2017).

Interestingly, $\delta^{13}C_{TCE}$ in the wells that also contained CF ranged between -32.5 and -31.8‰ but was significantly enriched in ^{13}C in the unique well (PI-3) that lacked CF ($\delta^{13}C_{TCE}$ = -28.2‰, Figure 1A). This may be in agreement with several studies suggesting that CF can inhibit significantly microbial reductive dechlorination of CEs, as reviewed elsewhere (Wei et al., 2016). However, *cis*-DCE, VC and ETH were also detected in most of the monitored wells (SI section G) indicating that, despite this potential inhibition effect suggested by the isotopic analysis, full dechlorination of TCE occurred.

Lastly, no significant carbon isotope fractionation was observed for MCB ($\Delta\delta^{13}C_{MCB}$ < 2‰, SI section H), and obtained $\delta^{13}C$ values were within the available range of commercial MCB solvents (Table 2), indicating that this compound was, most likely, not being degraded.

To investigate the biodegradation potential of the site, three different microcosm treatments were prepared with groundwater from well PI-2 (SI section J). The non-amended microcosms used as natural attenuation controls fully degraded CF and DCM, and transformed TCE to VC after 75 days. The microcosms amended with either only lactate (biostimulation) or also inoculated with "S" (bioaugmentation) increased the degradation rate of CF (to DCM), DCM, TCE and, more importantly, fully dechlorinated the latter to stoichiometric amounts of ETH. Both CMs and CEs elimination occurred

simultaneously (SI section J). These results confirmed the feasibility of *in-situ* CF, DCM and TCE biodegradation, and agreed with the information obtained from the isotopic field data that was just discussed. In contrast, MCB always accumulated in the medium of the microcosms and was not degraded (SI section J). Such evidence further supports the evidence obtained from the isotopic field data, which pointed towards the recalcitrance of the pollutant. Thus, it could be discarded that benzene, which was detected in the preliminary characterization of this aquifer, was derived from MCB biodegradation. Regarding the amended substrate, lactate was converted to acetate (major product) and propionate in all the amended microcosms (SI section K).

The composition of the microbial community was assessed by 16S rRNA high-throughput sequencing. The analysis was performed on groundwater samples collected from well PI-2 that were enriched with CF for four consecutive dilution series. The taxonomic assignments of 16S rRNA sequences revealed that the four predominant genera were *Clostridium* (31%), *Sedimentibacter* (25%), *Dehalobacter* (10%) and *Acetobacterium* (4%) (SI section L). The presence of *Dehalobacter*, a well-known CF and DCM degrader (Justicia-Leon et al., 2012; Lee et al., 2015), further supports the intrinsic biodegradation potential of the aquifer to remediate CMs. In addition, results also suggested that *Clostridium* sp. and *Acetobacterium* sp. could be somehow involved in the degradation of CF as well, as described elsewhere (Egli et al., 1990, 1988; Gälli and McCarty, 1989; Wanner et al., 2018).

With these evidences and aiming to better understand the origin and fate of CF and DCM at this site, a dual C–Cl isotopic assessment was performed based on the assumption that CF in well CV-5 reflected the initial isotopic signature (CF_0) since it possessed the most depleted $\delta^{13}C$ and $\delta^{37}Cl$ values (Figure 1A). The dual isotope fractionation pattern observed for CF in CV-3, PI-17 and PI-26 was consistent with the degradation of leaked

commercial CF, since the data points fell within the estimated potential isotopic composition for degraded CF (orange area, Figure 1B). Accordingly, the values for DCM initially produced from CF degradation (DCM_{ini}) ranged between -50.9‰ and -73.9‰ for $\delta^{13}C$ and was of -2.2‰ for $\delta^{37}Cl$ (Figure 1B, SI section E). The isotopic composition of DCM detected in well PI-26 (SI section H) was enriched in ^{37}Cl compared to that of commercial DCM (Table 2), and in both ^{13}C and ^{37}Cl compared to that of DCM produced by CF degradation (SI section E), suggesting that it could be subject to biodegradation (Figure 1B). However, regarding the main source of detected DCM at the site, obtained results point to a potential spill of DCM at the site being more likely than DCM produced by CF degradation, but neither could be confirmed.

In the above scenario, and assuming *Dehalobacter* sp. was the responsible for CF biotransformation, the extent of biodegradation (D%) for CF estimated in the wells CV-3, PI-17 and PI-26 (where $\Delta\delta^{13}C$ was > 2‰, SI section H) ranged between 7–11% considering the εC data reported for *Dehalobacter* strain CF (εC = -28 ± 2)). Data for *Dehalobacter* strain CF was used for this calculation because its $\Lambda^{C/Cl}$ was more coherent with the field results from Site 1 (i.e. the isotopic pattern of positive dual C–Cl slopes observed for CF measurements), than the $\Lambda^{C/Cl}$ of *Dehalobacter* strain UNSWDHB (Table 1). Nevertheless, further research needs to be done on this culture to better understand the roles of *Dehalobacter*, *Clostridium* and *Acetobacterium* bacteria, and elucidate the biodegradation mechanisms of both CF and DCM, which would allow an improved assessment and quantification of D% at the field.

3.3.2. Site 2

At this site, Eh ranged from +254 to -118 mV, but groundwater in most of the wells exhibited oxic conditions which limit the occurrence of reductive dechlorination reactions (SI section F). Temperature and pH were considered homogeneous and averaged 24 ± 2

ºC and 6.8 ± 0.3, respectively (SI section F). CF was detected at the highest concentrations (272 mg/L), followed by DCM (27 mg/L), TCE (1.7 mg/L) and MCB (0.88 mg/L) (Figure 2A and SI section G).

$\delta^{13}C$ and $\delta^{37}Cl$ of CF could be determined in 7 out of 9 wells because the concentration of CF in PZ-5 and PZ-31 was below the limit of quantification (Figure 2A). The $\Delta\delta^{13}C_{CF}$ > 2‰ observed between PZ-9 and PZ-18 wells and the $\Delta\delta^{37}Cl_{CF}$ < 2‰ observed between PZ-10 and PZ-18 wells (SI section H) could be related to CF transformation in groundwater (Hunkeler et al., 2008) considering the low εCl reported for CF transformation. However, most of the C–Cl isotope compositions of CF were within the isotopic range for commercial CF (SI section I), which could also indicate that measured $\delta^{13}C$ and $\delta^{37}Cl$ belonged to a leaked and not degraded CF.

On its side, detected DCM presented a higher variation for both C and Cl isotope ratios ($\Delta\delta^{13}C_{DCM}$ = 6.1‰ between wells PZ-19 and PZ-36, $\Delta\delta^{37}Cl_{DCM}$ = 2.2‰ between wells PZ-9 and PZ-18, Figure 2A, SI section H) indicative of potential *in-situ* transformations. In this case, however, the isotopic composition in well PZ-36 did fall within the commercial DCM, whereas well PZ-19 did not (Figure 2B and SI section I, see further discussion below).

For TCE, $\Delta\delta^{13}C$ was of 5.8‰ (SI section H), which could be related to TCE transformation in groundwater (Hunkeler et al., 2008), and measured $\delta^{13}C_{TCE}$ values were more enriched in ^{13}C than the $\delta^{13}C$ compositions of commercial TCE (Table 2), in agreement with potential TCE degradation. However, the reductive dechlorination products of TCE (DCE, VC, and ETH) were detected occasionally and at very low concentrations (SI section G).

Microcosm experiments were prepared with groundwater from wells PZ-9, PZ-19 and

494 PZ-36. Microcosms for well PZ-9 did not show significant degradation of neither CF nor
495 CEs, and no major differences were observed between the non-amended, biostimulated
496 and the bioaugmented treatments after 150 days (SI section M). However, traces of DCM
497 and VC, a slight decrease in PCE and TCE, and formation of *trans*-DCE were observed
498 throughout the course of the study (SI section M). For PZ-19, no significant elimination
499 of contaminants was observed, although TCE did exhibit a decrease in all microcosms
500 and traces of *cis*-DCE, *trans*-DCE and VC were detected in some of them (SI section N).
501 For PZ-36, the non-amended, biostimulated and bioaugmented (with "M") microcosms
502 did neither degrade CF nor CEs significantly. In contrast, the bioaugmented (with "S")
503 treatment exhibited a CF decrease with the transient production of DCM, and TCE was
504 completely transformed to VC and *trans*-DCE (SI section O). Amended lactate was
505 mainly transformed to acetate in PZ-9 and PZ-36 microcosms. In PZ-19, however, lactate
506 was not completely consumed but, in both bioaugmentation tests, its decrease was
507 followed by acetate and propionate production (SI section K). The inability of inoculated
508 bacteria to efficiently degrade contaminants in these microcosms suggested that there
509 were inhibition issues, possibly due to the presence of co-contaminants in groundwater
510 such as CT, which is a known inhibitor of the microbial activity and CF degradation in
511 particular (section 2.2) (da Lima and Sleep, 2010; Grostern et al., 2010; Justicia-Leon et
512 al., 2014; Wei et al., 2016). The results obtained with the microcosms suggested that,
513 under the studied conditions, degradation of contaminants was very slow and inefficient,
514 but possible to some extent, which agreed with the information obtained from the isotopic
515 field data that was discussed above.

516 At this site, the dual C–Cl isotopic assessment was performed based on a CF_0 signature
517 of $\delta^{13}C$ = -45.1‰ (from PZ-9) and $\delta^{37}Cl$ = -3.5‰ (from PZ-10), as they were the most
518 depleted values measured (Figure 2A). The dual isotope fractionation pattern observed

519 for CF was not consistent with degradation (orange area, Figure 2B), in agreement with
520 the microcosms. However, it should be noted that $\delta^{37}Cl_{CF}$ values were enriched respect
521 to CF_0 signature. This could be attributable to Cl isotope fractionation processes in the
522 unsaturated zone due to diffusion-controlled vaporization (Jeannottat and Hunkeler,
523 2012; Palau et al., 2016) or to the leakage of CF from different providers with distinct
524 isotopic signatures. Moreover, it has to be taken into account that this release of CF was
525 still active at the site and potential CF degradation could be masked by a more depleted
526 CF input. In the hypothetical case that CF was biologically degraded, the calculated
527 isotopic range for DCM_{ini} (formation of DCM from CF degradation) would range from -
528 52.1‰ to -75.1‰ for carbon, and -3.5‰ for chlorine (Figure 2B, SI section E). The
529 isotopic composition of DCM detected in groundwater (Figure 2B, SI section H) was very
530 enriched in both ^{37}Cl and ^{13}C compared to that of initial DCM produced by CF
531 degradation (grey area, Figure 2B). In detail, DCM detected in PZ-36 (with the highest
532 DCM concentration, Figure 2A) was within the range of commercial DCM (Figure 2B),
533 pointing to a potential release of DCM at the site. However, this DCM could be subject
534 to a little biodegradation as acetate, the main by-product of DCM fermentation, was
535 detected in the well PZ-36 and also in PZ-18 (SI section G). For the well PZ-19, the
536 $\delta^{13}C_{DCM}$ value is slightly depleted in ^{13}C while the $\delta^{37}Cl_{DCM}$ value is lightly enriched in
537 ^{37}Cl compared to those measured in PZ-36 (Figure 2B). This could be explained similar
538 to CF, in this case DCM could be an impurity in the CF raw source with isotopic signature
539 changing over time due to change in CF providers or manufacturing processes or by the
540 effect of vaporization and diffusion processes in the unsaturated zone (Jeannottat and
541 Hunkeler, 2012; Palau et al., 2016). As noted above, the release of CF (and probably
542 DCM) was still active at the site. Taking all these evidences into account, the extent of
543 biodegradation (D%) for CF was not estimated since the results would not be

representative of CF degradation.

4. Conclusions

The present study provides additional data on isotope C and Cl compositions for different commercial CMs, widening the known range for these solvents and proving the utility of these results for data interpretation. In addition, the C and Cl isotopic fractionation values for the anaerobic degradation of DCM by a *Dhb*-containing culture were also determined. These results enrich the available database that can be used by practitioners to provide diagnostic information about CMs biodegradation in contaminated aquifers. The value of $\Lambda^{C/Cl}$ obtained for the investigated *Dhb*-containing culture was right in between of those described for *Dhb f.* and D. elyunquensis, which would allow the distinction of these DCM degradation mechanisms through isotope analyses.

The pumping regimes that were active at both studied sites probably impacted the geographical distribution of the chlorinated compounds and their corresponding isotopic signatures. For this reason, the focus of this work was not on the flow path of the plume but on the correlation between the isotopic composition of the chlorinated solvents and the biodegradation information obtained from microcosms experiments for each monitoring well. For this, the use of an integrative approach that combines C–Cl CSIA, laboratory microcosms, and 16S rRNA high-throughput sequencing demonstrated the intrinsic biodegradation potential of Site 1 to fully transform CF, DCM, and CEs, but not MCB. In contrast, results for Site 2 suggested that inhibition was preventing the efficient elimination of CMs and CEs at tested conditions. Nevertheless, the dual C–Cl isotopic assessment proved useful, as well, to elucidate the origin and fate of DCM and CF at both

sites. Considering these results, a biostimulation (e.g. enhanced reductive dechlorination with lactate) could be applied at Site 1 to degrade both CMs and CEs. However, the persistence of MCB at this site, and the inhibition of biodegradation observed at Site 2, suggest that a treatment train (i.e. a combination or sequence of different remedial strategies targeting different groups of contaminants) could possibly be the optimal approach for the detoxification of these aquifers.

This study shows that such a multi-method approach allows for the collection of data that can help making decisions in the field. In this case, it is a valuable tool to evaluate the feasibility of biodegradation strategies to remediate chlorinated solvents in complex multi-contaminated aquifers, as it can provide the lines of evidence required to demonstrate whether bacteria can successfully detoxify groundwater, and identify any potential setbacks. The microcosm tests can provide a positive indication that complete dechlorination can be achieved by native microbial populations, and is useful to predict the effect of bioremediation treatments (biostimulation or bioaugmentation) to detoxify the aquifer. Changes in carbon and chlorine isotope composition among the residual fraction of the chlorinated compounds in the monitoring wells can provide field evidence for microbial degradation. Lastly, the positive molecular identification of key organohalide-respiring bacteria (e.g. *Dehalobacter*) can provide additional evidence that chlorinated solvents can be fully dechlorinated in the aquifer. Notwithstanding, there is a need for additional laboratory studies that correlate the metabolism of microbial transformations with stable isotope fractionation of multiple elements to support the interpretation of CSIA data obtained from contaminated groundwaters, as well as the potential inhibitory effect of co-contaminants over bacteria degrading organochlorides.

5. Acknowledgements

593 This research has been supported by the Spanish State Research Agency (CTM2016-
594 75587-C2-1-R and CGL2017-87216-C4-1-R projects), co-financed by the European
595 Union through the European Regional Development Fund (ERDF). This work was also
596 partly supported by *Generalitat de Catalunya* through the consolidate research groups
597 (2017SGR-14 and 2017SGR-1733) and the Industrial Doctorate grant of N. Blázquez-
598 Pallí (2015-DI-064). A. Trueba-Santiso acknowledges support from a MICINN
599 predoctoral research grant (BES-2014-070817). M. Rosell acknowledges a *Ramón y*
600 *Cajal* contract (RYC-2012-11920) from MICINN. The *Departament d'Enginyeria*
601 *Química, Biològica i Ambiental* of *Universitat Autònoma de Barcelona* is a member of
602 the *Xarxa de Referència en Biotecnologia de la Generalitat de Catalunya*. The authors
603 thank Jesica M. Soder-Walz for her collaboration in the laboratory work.

References

Aelion, C.M., Höhener, P., Hunkeler, D., Aravena, R., 2009. Environmental Isotopes in Bioremediation and Biodegradation. CRC Press, Boca Raton. https://doi.org/10.1159/000076616

Aeppli, C., Berg, M., Cirpka, O.A., Holliger, C., Schwarzenbach, R.P., Hofstetter, T.B., 2009. Influence of mass-transfer limitations on carbon isotope fractionation during microbial dechlorination of trichloroethene. Environ. Sci. Technol. 43, 8813–8820. https://doi.org/10.1021/es901481b

ATSDR, 2016. Substance priority list [WWW Document]. Subst. Prior. List. URL https://www.atsdr.cdc.gov/SPL/index.html (accessed 10.31.17).

Badin, A., Broholm, M.M., Jacobsen, C.S., Palau, J., Dennis, P., Hunkeler, D., 2016. Identification of abiotic and biotic reductive dechlorination in a chlorinated ethene plume after thermal source remediation by means of isotopic and molecular biology tools. J. Contam. Hydrol. 192, 1–19. https://doi.org/10.1016/j.jconhyd.2016.05.003

Badin, A., Buttet, G., Maillard, J., Holliger, C., Hunkeler, D., 2014. Multiple dual C–Cl isotope patterns associated with reductive dechlorination of tetrachloroethene. Environ. Sci. Technol. 48, 9179–9186. https://doi.org/10.1021/es500822d

Blázquez-Pallí, N., Rosell, M., Varias, J., Bosch, M., Soler, A., Vicent, T., Marco-Urrea, E., 2019. Multi-method assessment of the intrinsic biodegradation potential of an aquifer contaminated with chlorinated ethenes at an industrial area in Barcelona (Spain). Environ. Pollut. 244, 165–173. https://doi.org/10.1016/j.envpol.2018.10.013

Breider, F., 2013. Investigating the origin of chloroform in soils and groundwater using

carbon and chlorine stable isotopes analysis. Université de Neuchâtel (Switzerland).

Breider, F., Hunkeler, D., 2014. Investigating chloroperoxidase-catalyzed formation of chloroform from humic substances using stable chlorine isotope analysis. Environ. Sci. Technol. 48, 1592–1600. https://doi.org/10.1021/es403879e

Chan, C.C.H., Mundle, S.O.C., Eckert, T., Liang, X., Tang, S., Lacrampe-Couloume, G., Edwards, E., Sherwood Lollar, B., 2012. Large carbon isotope fractionation during biodegradation of chloroform by Dehalobacter cultures. Environ. Sci. Technol. 46, 10154–10160. https://doi.org/10.1021/es3010317

Chen, G., Kleindienst, S., Griffiths, D.R., Mack, E.E., Seger, E.S., Löffler, F.E., 2017. Mutualistic interaction between dichloromethane- and chloromethane-degrading bacteria in an anaerobic mixed culture. Environ. Microbiol. 19, 4784–4796. https://doi.org/10.1111/1462-2920.13945

Chen, G., Shouakar-Stash, O., Phillips, E., Justicia-Leon, S.D., Gilevska, T., Sherwood Lollar, B., Mack, E.E., Seger, E.S., Löffler, F.E., 2018. Dual carbon-chlorine isotope analysis indicates distinct anaerobic dichloromethane degradation pathways in two members of the Peptococcaceae. Environ. Sci. Technol. 52, 8607–8616. https://doi.org/10.1021/acs.est.8b01583

Cichocka, D., Siegert, M., Imfeld, G.G., Andert, J., Beck, K., Diekert, G., Richnow, H.H., Nijenhuis, I., 2007. Factors controlling the carbon isotope fractionation of tetra- and trichloroethene during reductive dechlorination by Sulfurospirillum ssp. and Desulfitobacterium sp. strain PCE-S. FEMS Microbiol. Ecol. 62, 98–107. https://doi.org/10.1111/j.1574-6941.2007.00367.x

Coplen, T.B., 2011. Guidelines and recommended terms for expression of stable-isotope-ratio and gas-ratio measurement results. Rapid Commun. Mass Spectrom. 25, 2538–

651 2560. https://doi.org/10.1002/rcm.5129

652 Coplen, T.B., 1996. New guidelines for reporting stable hydrogen, carbon, and oxygen
653 isotope-ratio data. Geochim. Cosmochim. Acta 60, 3359–3360.
654 https://doi.org/10.1016/0016-7037(96)00263-3

655 da Lima, G.P., Sleep, B.E., 2010. The impact of carbon tetrachloride on an anaerobic
656 methanol-degrading microbial community. Water. Air. Soil Pollut. 212, 357–368.
657 https://doi.org/10.1007/s11270-010-0350-z

658 Ding, C., Zhao, S., He, J., 2014. A Desulfitobacterium sp. strain PR reductively
659 dechlorinates both 1,1,1-trichloroethane and chloroform. Environ. Microbiol. 16,
660 3387–3397. https://doi.org/10.1111/1462-2920.12387

661 Egli, C., Stromeyer, S., Cook, A.M., Leisinger, T., 1990. Transformation of tetra- and
662 trichloromethane to CO2 by anaerobic bacteria is a non-enzymic process. FEMS
663 Microbiol. Lett. 68, 207–212. https://doi.org/10.1016/0378-1097(90)90152-G

664 Egli, C., Tschan, T., Scholtz, R., Cook, A.M., Leisinger, T., 1988. Transformation of
665 tetrachloromethane to dichloromethane and carbon-dioxide by Acetobacterium-
666 Woodii. Appl. Environ. Microbiol. 54, 2819–2824.

667 Elsner, M., 2010. Stable isotope fractionation to investigate natural transformation
668 mechanisms of organic contaminants: principles, prospects and limitations. J.
669 Environ. Monit. 12, 2005–2031. https://doi.org/10.1039/c0em00277a

670 European Commission, 2012. Priority Substances and Certain Other Pollutants according
671 to Annex II of Directive 2008/105/EC [WWW Document]. URL
672 http://ec.europa.eu/environment/water/water-framework/priority_substances.htm
673 (accessed 10.31.17).

674 Gälli, R., McCarty, P.L., 1989. Biotransformation of 1,1,1-trichloroethane,
675 trichloromethane, and tetrachloromethane by a Clostridium sp. Appl. Environ.
676 Microbiol. 55, 837–844.

677 Gribble, G.W., 2010. Naturally Occurring Organohalogen Compounds - A
678 Comprehensive Update, Asian Journal of WTO and International Health Law and
679 Policy, Fortschritte der Chemie organischer Naturstoffe / Progress in the Chemistry
680 of Organic Natural Products. Springer Vienna, Vienna. https://doi.org/10.1007/978-
681 3-211-99323-1

682 Grostern, A., Duhamel, M., Dworatzek, S., Edwards, E., 2010. Chloroform respiration to
683 dichloromethane by a Dehalobacter population. Environ. Microbiol. 12, 1053–1060.
684 https://doi.org/10.1111/j.1462-2920.2009.02150.x

685 Heckel, B., Cretnik, S., Kliegman, S., Shouakar-Stash, O., McNeill, K., Elsner, M.,
686 2017a. Reductive outer-sphere single electron transfer is an exception rather than the
687 rule in natural and engineered chlorinated ethene dehalogenation. Environ. Sci.
688 Technol. 51, 9663–9673. https://doi.org/10.1021/acs.est.7b01447

689 Heckel, B., Phillips, E., Edwards, E., Sherwood Lollar, B., Elsner, M., Manefield, M.J.,
690 Lee, M., 2019. Reductive dehalogenation of trichloromethane by two different
691 Dehalobacter restrictus strains reveal opposing dual element isotope effects.
692 Environ. Sci. Technol. 53, 2332–2343. https://doi.org/10.1021/acs.est.8b03717

693 Heckel, B., Rodríguez-Fernández, D., Torrentó, C., Meyer, A.H., Palau, J., Domènech,
694 C., Rosell, M., Soler, A., Hunkeler, D., Elsner, M., 2017b. Compound-specific
695 chlorine isotope analysis of tetrachloromethane and trichloromethane by gas
696 chromatography-isotope ratio mass spectrometry vs gas chromatography-
697 quadrupole mass spectrometry: method development and evaluation of precision and

trueness. Anal. Chem. 89, 3411–3420. https://doi.org/10.1021/acs.analchem.6b04129

Heraty, L.J., Fuller, M.., Huang, L., Abrajano, T., Sturchio, N.., 1999. Isotopic fractionation of carbon and chlorine by microbial degradation of dichloromethane. Org. Geochem. 30, 793–799. https://doi.org/10.1016/S0146-6380(99)00062-5

Hermon, L., Denonfoux, J., Hellal, J., Joulian, C., Ferreira, S., Vuilleumier, S., Imfeld, G., 2018. Dichloromethane biodegradation in multi-contaminated groundwater: Insights from biomolecular and compound-specific isotope analyses. Water Res. 142, 217–226. https://doi.org/10.1016/j.watres.2018.05.057

Holt, B.D., Sturchio, N.C., Abrajano, T., Heraty, L.J., 1997. Conversion of chlorinated volatile organic compounds to carbon dioxide and methyl chloride for isotopic analysis of carbon and chlorine. Anal. Chem. 69, 2727–2733. https://doi.org/10.1021/ac961096b

Hunkeler, D., Meckenstock, R.U., Lollar, B.S., Schmidt, T.C., Wilson, J.T., 2008. A guide for assessing biodegradation and source identification of organic ground water contaminants using compound specific isotope analysis (CSIA), U.S. Environmental Protection Agency. Washington, D.C., EPA/600/R-08/148.

Hunkeler, D., Van Breukelen, B.M., Elsner, M., 2009. Modeling chlorine isotope trends during sequential transformation of chlorinated ethenes. Environ. Sci. Technol. 43, 6750–6756. https://doi.org/10.1021/es900579z

IARC, 2018. List of classifications, Volumes 1-122 [WWW Document]. IARC Monogr. Eval. Carcinog. Risks to Humans. URL https://monographs.iarc.fr/list-of-classifications-volumes/ (accessed 10.6.18).

721 IARC, 2016. Some chemicals used as solvents and in polymer manufacture, IARC
722 Monographs on the Evaluation of Carcinogenic Risks to Humans. Lyon.

723 Jeannottat, S., Hunkeler, D., 2012. Chlorine and carbon isotopes fractionation during
724 volatilization and diffusive transport of trichloroethene in the unsaturated zone.
725 Environ. Sci. Technol. 46, 3169–3176. https://doi.org/10.1021/es203547p

726 Jendrzejewski, N., Eggenkamp, H.G.M., Coleman, M.. L., 2001. Characterisation of
727 chlorinated hydrocarbons from chlorine and carbon isotopic compositions: Scope of
728 application to environmental problems. Appl. Geochemistry 16, 1021–1031.
729 https://doi.org/10.1016/S0883-2927(00)00083-4

730 Justicia-Leon, S.D., Higgins, S., Mack, E.E., Griffiths, D.R., Tang, S., Edwards, E.,
731 Löffler, F.E., 2014. Bioaugmentation with distinct Dehalobacter strains achieves
732 chloroform detoxification in microcosms. Environ. Sci. Technol. 48, 1851–1858.
733 https://doi.org/10.1021/es403582f

734 Justicia-Leon, S.D., Ritalahti, K.M., Mack, E.E., Löffler, F.E., 2012. Dichloromethane
735 fermentation by a Dehalobacter sp. in an enrichment culture derived from pristine
736 river sediment. Appl. Environ. Microbiol. 78, 1288–1291.
737 https://doi.org/10.1128/AEM.07325-11

738 Kampara, M., Thullner, M., Richnow, H.H., Harms, H., Wick, L.Y., 2008. Impact of
739 bioavailability restrictions on microbially induced stable isotope fractionation. 2.
740 Experimental evidence. Environ. Sci. Technol. 42, 6552–6558.
741 https://doi.org/10.1021/es702781x

742 Kaufmann, R., Long, A., Bentley, H., Davis, S., 1984. Natural chlorine isotope variations.
743 Nature 309, 338–340. https://doi.org/10.1038/309338a0

744 Kleindienst, S., Chourey, K., Chen, G., Murdoch, R.W., Higgins, S.A., Iyer, R.,
745 Campagna, S.R., Mack, E.E., Seger, E.S., Hettich, R.L., Löffler, F.E., 2019.
746 Proteogenomics reveals novel reductive dehalogenases and methyltransferases
747 expressed during anaerobic dichloromethane metabolism. Appl. Environ. Microbiol.
748 85. https://doi.org/10.1128/AEM.02768-18

749 Kleindienst, S., Higgins, S.A., Tsementzi, D., Chen, G., Konstantinidis, K.T., Mack, E.E.,
750 Löffler, F.E., 2017. 'Candidatus Dichloromethanomonas elyunquensis' gen. nov.,
751 sp. nov., a dichloromethane-degrading anaerobe of the Peptococcaceae family. Syst.
752 Appl. Microbiol. 40, 150–159. https://doi.org/10.1016/j.syapm.2016.12.001

753 Klindworth, A., Pruesse, E., Schweer, T., Peplies, J., Quast, C., Horn, M., Glöckner, F.O.,
754 2013. Evaluation of general 16S ribosomal RNA gene PCR primers for classical and
755 next-generation sequencing-based diversity studies. Nucleic Acids Res. 41, e1–e1.
756 https://doi.org/10.1093/nar/gks808

757 Krone, U., Laufer, K., Thauer, R.K., Hogenkamp, H.P.C., 1989a. Coenzyme F430 as a
758 possible catalyst for the reductive dehalogenation of chlorinated C1 hydrocarbons in
759 methanogenic bacteria. Biochemistry 28, 10061–10065.
760 https://doi.org/10.1021/bi00452a027

761 Krone, U., Thauer, R.K., Hogenkamp, H.P.C., 1989b. Reductive dehalogenation of
762 chlorinated C1-hydrocarbons mediated by corrinoids. Biochemistry 28, 4908–4914.
763 https://doi.org/10.1021/bi00437a057

764 Lee, M., Low, A., Zemb, O., Koenig, J., Michaelsen, A., Manefield, M.J., 2012. Complete
765 chloroform dechlorination by organochlorine respiration and fermentation. Environ.
766 Microbiol. 14, 883–894. https://doi.org/10.1111/j.1462-2920.2011.02656.x

767 Lee, M., Wells, E., Wong, Y.K., Koenig, J., Adrian, L., Richnow, H.H., Manefield, M.J.,

768 2015. Relative contributions of dehalobacter and zerovalent iron in the degradation
769 of chlorinated methanes. Environ. Sci. Technol. 49, 4481–4489.
770 https://doi.org/10.1021/es5052364

771 Liang, X., Howlett, M.R., Nelson, J.L., Grant, G., Dworatzek, S., Lacrampe-Couloume,
772 G., Zinder, S.H., Edwards, E., Sherwood Lollar, B., 2011. Pathway-dependent
773 isotope fractionation during aerobic and anaerobic degradation of
774 monochlorobenzene and 1,2,4-trichlorobenzene. Environ. Sci. Technol. 45, 8321–
775 8327. https://doi.org/10.1021/es201224x

776 Löffler, F.E., Sanford, R.A., Ritalahti, K.M., 2005. Enrichment, cultivation, and detection
777 of reductively dechlorinating bacteria. Methods Enzymol. 397, 77–111.
778 https://doi.org/10.1016/S0076-6879(05)97005-5

779 Mägli, A., Messmer, M., Leisinger, T., 1998. Metabolism of dichloromethane by the strict
780 anaerobe Dehalobacterium formicoaceticum. Appl. Environ. Microbiol. 64, 646–
781 650.

782 Marshall, K.A., Pottenger, L.H., 2016. Chlorocarbons and Chlorohydrocarbons, in: Ley,
783 C. (Ed) Kirk-Othmer Encyclopedia of Chemical Technology. John Wiley & Sons,
784 Inc., Hoboken, NJ, USA, pp. 1–29.
785 https://doi.org/10.1002/0471238961.1921182218050504.a01.pub3

786 Martín-González, L., Mortan, S.H., Rosell, M., Parladé, E., Martínez-Alonso, M., Gaju,
787 N., Caminal, G., Adrian, L., Marco-Urrea, E., 2015. Stable carbon isotope
788 fractionation during 1,2-dichloropropane-to-propene transformation by an
789 enrichment culture containing Dehalogenimonas strains and a dcpA gene. Environ.
790 Sci. Technol. 49, 8666–74. https://doi.org/10.1021/acs.est.5b00929

791 Mikesell, M.D., Boyd, S.A., 1990. Dechlorination of chloroform by Methanosarcina

792 strains. Appl. Environ. Microbiol. 56, 1198–1201.

793 Mortan, S.H., Martín-González, L., Vicent, T., Caminal, G., Nijenhuis, I., Adrian, L.,
794 Marco-Urrea, E., 2017. Detoxification of 1,1,2-trichloroethane to ethene in a
795 bioreactor co-culture of Dehalogenimonas and Dehalococcoides mccartyi strains. J.
796 Hazard. Mater. 331, 218–225. https://doi.org/10.1016/j.jhazmat.2017.02.043

797 Muller, E.E.L., Bringel, F., Vuilleumier, S., 2011. Dichloromethane-degrading bacteria
798 in the genomic age. Res. Microbiol. 162, 869–876.
799 https://doi.org/10.1016/j.resmic.2011.01.008

800 Mundle, S.O.C., Vandersteen, A.A., Lacrampe-Couloume, G., Kluger, R., Sherwood
801 Lollar, B., 2013. Pressure-monitored headspace analysis combined with compound-
802 specific isotope analysis to measure isotope fractionation in gas-producing reactions.
803 Rapid Commun. Mass Spectrom. 27, 1778–1784. https://doi.org/10.1002/rcm.6625

804 Nikolausz, M., Nijenhuis, I., Ziller, K., Richnow, H.H., Kastner, M., 2006. Stable carbon
805 isotope fractionation during degradation of dichloromethane by methylotrophic
806 bacteria. Environ. Microbiol. 8, 156–164. https://doi.org/10.1111/j.1462-
807 2920.2005.00878.x

808 Palau, J., Jamin, P., Badin, A., Vanhecke, N., Haerens, B., Brouyère, S., Hunkeler, D.,
809 2016. Use of dual carbon–chlorine isotope analysis to assess the degradation
810 pathways of 1,1,1-trichloroethane in groundwater. Water Res. 92, 235–243.
811 https://doi.org/10.1016/j.watres.2016.01.057

812 Palau, J., Yu, R., Mortan, S.H., Shouakar-Stash, O., Rosell, M., Freedman, D.L., Sbarbati,
813 C., Fiorenza, S., Aravena, R., Marco-Urrea, E., Elsner, M., Soler, A., Hunkeler, D.,
814 2017. Distinct dual C–Cl isotope fractionation patterns during anaerobic
815 biodegradation of 1,2-dichloroethane: potential to characterize microbial

816 degradation in the field. Environ. Sci. Technol. 51, 2685–2694.
817 https://doi.org/10.1021/acs.est.6b04998

818 Renpenning, J., Rapp, I., Nijenhuis, I., 2015. Substrate hydrophobicity and cell
819 composition influence the extent of rate limitation and masking of isotope
820 fractionation during microbial reductive dehalogenation of chlorinated ethenes.
821 Environ. Sci. Technol. 49, 4293–4301. https://doi.org/10.1021/es506108j

822 Rodríguez-Fernández, D., Torrentó, C., Guivernau, M., Viñas, M., Hunkeler, D., Soler,
823 A., Domènech, C., Rosell, M., 2018a. Vitamin B 12 effects on chlorinated methanes-
824 degrading microcosms: Dual isotope and metabolically active microbial populations
825 assessment. Sci. Total Environ. 621, 1615–1625.
826 https://doi.org/10.1016/j.scitotenv.2017.10.067

827 Rodríguez-Fernández, D., Torrentó, C., Palau, J., Marchesi, M., Soler, A., Hunkeler, D.,
828 Domènech, C., Rosell, M., 2018b. Unravelling long-term source removal effects and
829 chlorinated methanes natural attenuation processes by C and Cl stable isotopic
830 patterns at a complex field site. Sci. Total Environ. 645, 286–296.
831 https://doi.org/10.1016/j.scitotenv.2018.07.130

832 Sherwood Lollar, Barbara, Hirschorn, S., Mundle, S.O.C., Grostern, A., Edwards, E.,
833 Lacrampe-Couloume, G., Sherwood Lollar, B., 2010. Insights into enzyme kinetics
834 of chloroethane biodegradation using compound specific stable isotopes. Environ.
835 Sci. Technol. 44, 7498–7503. https://doi.org/10.1021/es101330r

836 Shouakar-Stash, O., Drimmie, R.J., Zhang, M., Frape, S.K., 2006. Compound-specific
837 chlorine isotope ratios of TCE, PCE and DCE isomers by direct injection using CF-
838 IRMS. Appl. Geochemistry 21, 766–781.
839 https://doi.org/10.1016/j.apgeochem.2006.02.006

840 Shouakar-Stash, O., Frape, S.K., Drimmie, R.J., 2003. Stable hydrogen, carbon and
841 chlorine isotope measurements of selected chlorinated organic solvents. J. Contam.
842 Hydrol. 60, 211–228. https://doi.org/10.1016/S0169-7722(02)00085-2

843 Tang, S., Edwards, E., 2013. Identification of Dehalobacter reductive dehalogenases that
844 catalyse dechlorination of chloroform, 1,1,1- trichloroethane and 1,1-
845 dichloroethane. Philos. Trans. R. Soc. B Biol. Sci. 368.
846 https://doi.org/10.1098/rstb.2012.0318

847 Thullner, M., Kampara, M., Richnow, H.H., Harms, H., Wick, L.Y., 2008. Impact of
848 bioavailability restrictions on microbially induced stable isotope fractionation. 1.
849 Theoretical calculation. Environ. Sci. Technol. 42, 6544–6551.
850 https://doi.org/10.1021/es702782c

851 Torgonskaya, M.L., Zyakun, A.M., Trotsenko, Y.A., Laurinavichius, K.S., Kümmel, S.,
852 Vuilleumier, S., Richnow, H.H., 2019. Individual stages of bacterial
853 dichloromethane degradation mapped by carbon and chlorine stable isotope analysis.
854 J. Environ. Sci. 78, 147–160. https://doi.org/10.1016/j.jes.2018.09.008

855 Torrentó, C., Palau, J., Rodríguez-Fernández, D., Heckel, B., Meyer, A., Domènech, C.,
856 Rosell, M., Soler, A., Elsner, M., Hunkeler, D., 2017. Carbon and chlorine isotope
857 fractionation patterns associated with different engineered chloroform
858 transformation reactions. Environ. Sci. Technol. 51, 6174–6184.
859 https://doi.org/10.1021/acs.est.7b00679

860 Trueba-Santiso, A., Parladé, E., Rosell, M., Lliros, M., Mortan, S.H., Martínez-Alonso,
861 M., Gaju, N., Martín-González, L., Vicent, T., Marco-Urrea, E., 2017. Molecular
862 and carbon isotopic characterization of an anaerobic stable enrichment culture
863 containing Dehalobacterium sp. during dichloromethane fermentation. Sci. Total

Environ. 581–582, 640–648. https://doi.org/10.1016/j.scitotenv.2016.12.174

van Warmerdam, E.M.M., Frape, S.K.K., Aravena, R., Drimmie, R.J., Flatt, H., Cherry, J.A. a, 1995. Stable chlorine and carbon isotope measurement of selected chlorinated organic solvents. Appl. Geochem. 10, 547–552. https://doi.org/10.1016/0883-2927(95)00025-9

Wanner, P., Parker, B.L., Chapman, S.W., Lima, G., Gilmore, A., Mack, E.E., Aravena, R., 2018. Identification of degradation pathways of chlorohydrocarbons in saturated low-permeability sediments using compound-specific isotope analysis. Environ. Sci. Technol. 52, 7296–7306. https://doi.org/10.1021/acs.est.8b01173

Weathers, L.J., Parkin, G.F., 2000. Toxicity of chloroform biotransformation to methanogenic bacteria. Environ. Sci. Technol. 34, 2764–2767. https://doi.org/10.1021/es990948x

Wei, K., Grostern, A., Chan, W.W.M., Richardson, R.E., Edwards, E.A., 2016. Electron acceptor interactions between organohalide-respiring bacteria: cross-feeding, competition, and inhibition, in: L. Adrian and F.E. Löffler (Ed) Organohalide-Respiring Bacteria. Springer Berlin Heidelberg, Berlin, Heidelberg, pp. 283–308. https://doi.org/10.1007/978-3-662-49875-0_13

Wong, Y.K., Holland, S.I., Ertan, H., Manefield, M.J., Lee, M., 2016. Isolation and characterization of Dehalobacter sp. strain UNSWDHB capable of chloroform and chlorinated ethane respiration. Environ. Microbiol. 18, 3092–3105. https://doi.org/10.1111/1462-2920.13287

887 **FIGURE AND CAPTIONS**

888

Figure 1. (A) Concentrations (in mg/L) and $\delta^{13}C$ and $\delta^{37}Cl$ compositions (in ‰) of CF, DCM, TCE and MCB from Site 1. Pie charts show the molar distribution of contaminants at each well. Detailed concentrations (in µM) and isotopic compositions are available in SI sections G and H, respectively. "n.d." means "could not be determined based on their low concentration"; "n.a." means "not analysed". (B) Dual C–Cl isotopic assessment for DCM and CF field data from Site 1. Both CF_0 and the range for DCM_{ini} are represented. Green and orange dashed rectangles depict the $\delta^{13}C$ and $\delta^{37}Cl$ ranges of commercial DCM and CF solvents, respectively (see Table 2 for details).

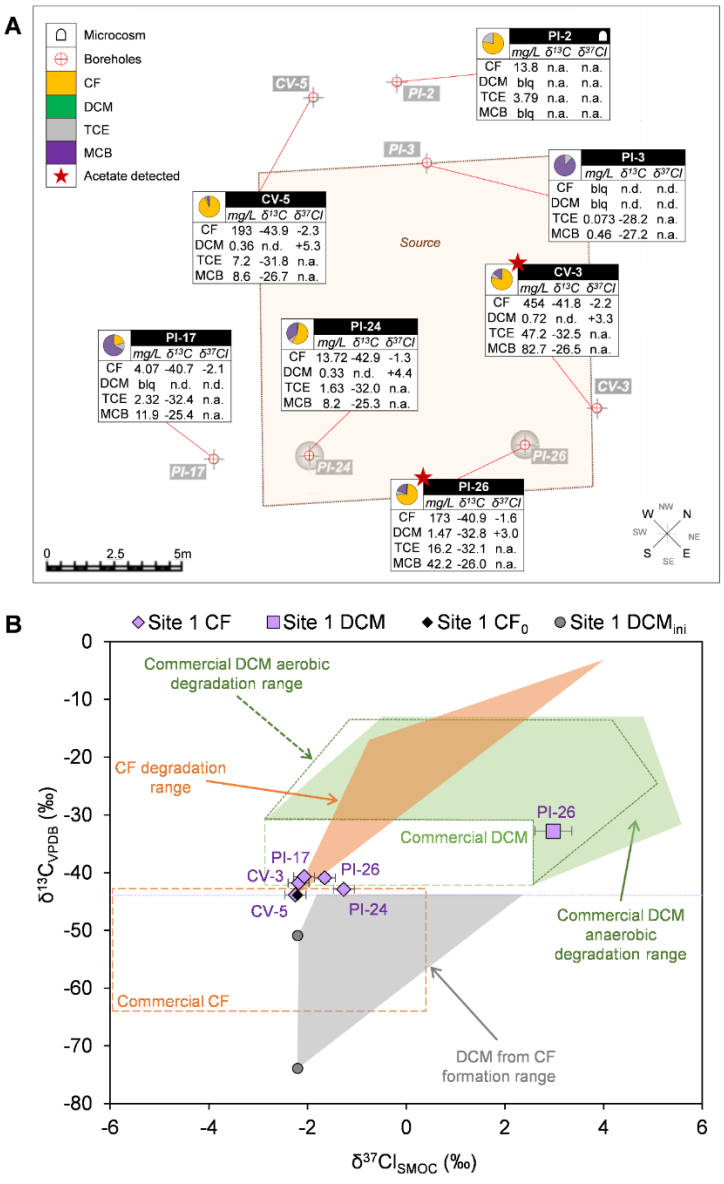

Figure 2. (A) Concentrations (in mg/L) and $\delta^{13}C$ and $\delta^{37}Cl$ compositions (in ‰) of CF, DCM, TCE and MCB from Site 2. Pie charts show the molar distribution of contaminants at each well. Detailed concentrations (in µM) and isotopic compositions are available in SI sections G and H, respectively. "n.d." means "could not be determined based on their low concentration"; "n.a." means "not analysed". (B) Dual C–Cl isotopic assessment for DCM and CF field data from Site 2. Both CF_0 and the range for DCM_{ini} are represented. Green and orange dashed rectangles depict the $\delta^{13}C$ and $\delta^{37}Cl$ ranges of commercial DCM and CF solvents, respectively (see Table 2 for details).

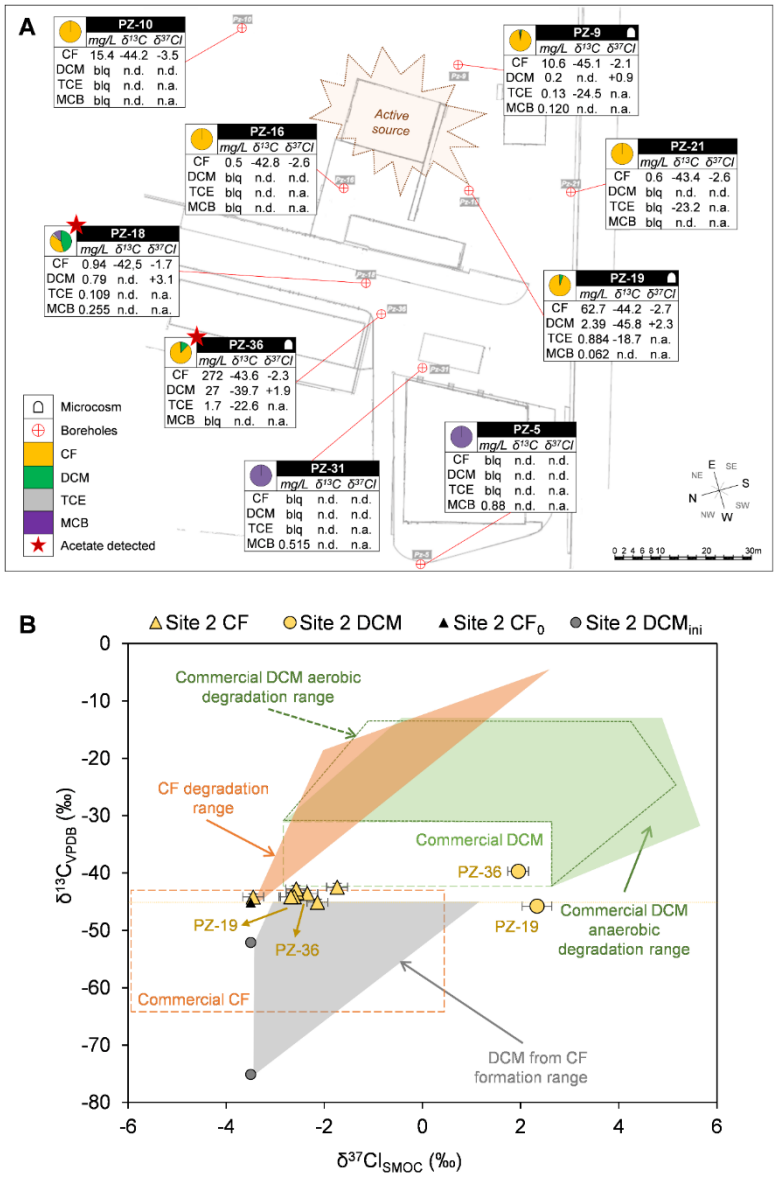

907 **Figure 3.** Double logarithmic Rayleigh plot for chlorine isotope data (A) and dual C–Cl
908 isotope plot (B) for the anaerobic degradation of DCM by the *Dhb* containing culture
909 investigated in this study. Solid black lines for the *Dhb* culture in each panel depict the
910 corresponding linear regression and dashed lines represent the associated 95% CI. In
911 panel B, the trend lines reported for DCM degradation by *Hyphomicrobium* strain MC8b
912 (Heraty et al., 1999), *Dhb f.* and D. elyunquensis (Chen et al., 2018) are shown for
913 comparison. Data points show the error bars from duplicate measurements.

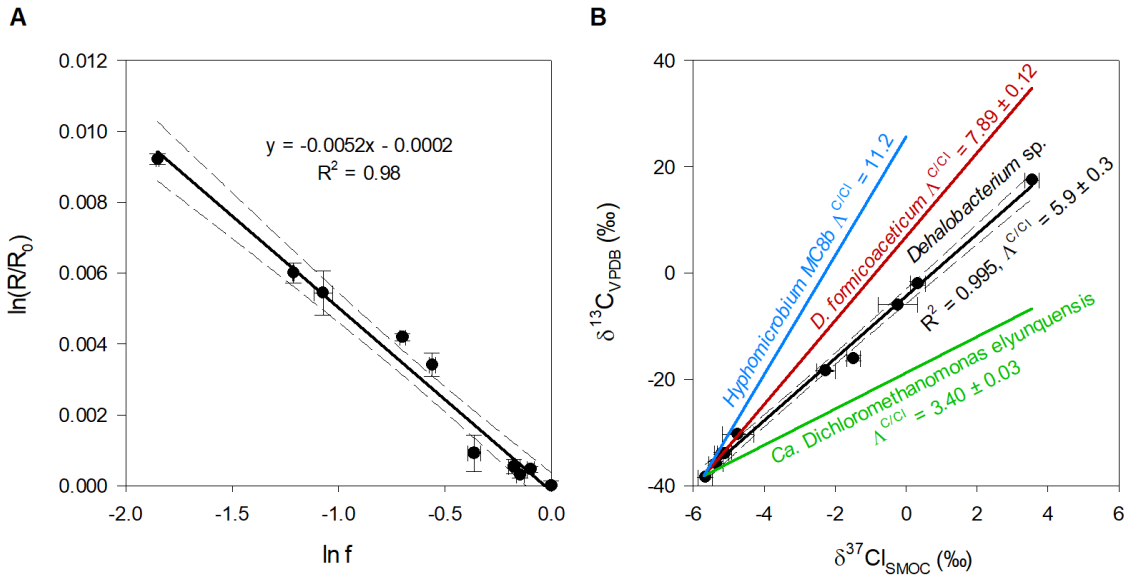

914

915

TABLES

Table 1. εC, εCl and $\Lambda^{C/Cl}$ of DCM and CF degradation by several mechanisms[a].

DCM	εC (‰)	εCl (‰)	$\Lambda^{C/Cl}$	Reference
Mixed culture containing *Dehalobacterium* sp. (*Dhb*)	-31 ± 3*	-5.2 ± 0.6	+5.9 ± 0.3	This study and re-calculated from Trueba-Santiso et al. (2017)*
Dehalobacterium formicoaceticum (*Dhb f.*)	-42.4 ± 0.7	-5.3 ± 0.1	+7.89 ± 0.12	Chen et al. (2018)
Consortium RM harboring *Ca.* Dichloromethanomonas elyunquensis	-18.3 ± 0.2	-5.2 ± 0.1	+3.40 ± 0.03	Chen et al. (2018)
Mixed culture containing *Dehalobacter* sp. (DCMD)	-16 ± 2	n.a.[b]	n.a.	Lee et al. (2015)
Hyphomicrobium sp. strain MC8b	-42.4[c,d]	-3.8[c,d]	+11.2[c,d]	Heraty et al. (1999)
Hyphomicrobium strains, *Methylobacterium*, *Methylopila*, *Methylophilus*, and *Methylorhabdus* strains	-41.2 to -66.3[d] -45.8 to -61.0[e]	n.a.	n.a.	Nikolausz et al. (2006) Nikolausz et al. (2006)
Hyphomicrobium strains	-22 to -46[d] -26 ± 5[e]	n.a.	n.a.	Hermon et al. (2018) Hermon et al. (2018)
Methylobacterium extorquens DM4 (average between high and low density cell suspensions)	-66.6[d,f]	-7.0[d,f]	+9.5[d,f]	Torgonskaya et al. (2019)
DM4 DCM dehalogenase (average between high and low activity)	-48.4[d,f]	-5.7[d,f]	+8.5[d,f]	Torgonskaya et al. (2019)
DM11 DCM dehalogenase (average between high and low activity)	-45.4[d,f]	-5.6[d,f]	+8.1[d,f]	Torgonskaya et al. (2019)
CF	**εC (‰)**	**εCl (‰)**	**$\Lambda^{C/Cl}$**	**Reference**
Oxidation	-8 ± 1	-0.44 ± 0.06	+17 ± 2	Torrentó et al. (2017)
Alkaline hydrolysis	-57 ± 5	-4.4 ± 0.4	+13.0 ± 0.8	Torrentó et al. (2017)
Hydrogenolysis plus reductive elimination with Fe (0)	-33 ± 11	-3 ± 1	+8 ± 2	Torrentó et al. (2017)
Biodegradation with vitamin B_{12}	-14 ± 4	-2.4 ± 0.4	+7 ± 1	Rodríguez-Fernández et al. (2018a)
Outer-sphere single electron transfer (OS-SET)	-17.7 ± 0.8	-2.6 ± 0.2	+6.7 ± 0.4	Heckel et al. (2017a)
Dehalobacter strain CF	-28 ± 2	-4.2 ± 0.2	+6.6 ± 0.1	Heckel et al. (2019)
Dehalobacter strain UNSWDHB	-3.1 ± 0.5	+2.5 ± 0.3	-1.2 ± 0.2	Heckel et al. (2019)
Mixed culture containing *Dehalobacter* strain UNSWDHB	-4.3 ± 0.5	n.a.	n.a.	Lee et al. (2015)

[a]Uncertainties of ε and Λ values correspond to the 95% confidence interval (CI). [b]n.a., values were not analysed. [c]$\Lambda^{C/Cl}$ values were calculated based on reported εC and εCl data by the referenced authors. [d]Values were measured under oxic conditions. [e]Values were measured under nitrate-reducing conditions. [f]εC and εCl values were calculated here based on reported αC and αCl data ($\varepsilon_{C,Cl} = 1/\alpha_{C,Cl} - 1) \cdot 1000$), and the $\Lambda^{C/Cl}$ values from the here estimated εC and εCl values ($\Lambda^{C/Cl} \sim \varepsilon_C/\varepsilon_{Cl}$).

919 **Table 2**. $\delta^{13}C$ and $\delta^{37}Cl$ (in ‰) of commercial pure-phase CF, DCM, TCE and MCB.

DCM	**$\delta^{13}C$ (‰/VPDB)**	**$\delta^{37}Cl$ (‰/SMOC)**	**Reference**
Fisher	-41.71 ± 0.08	-2.7 ± 0.1	This study
Sigma Aldrich	-	+0.75 ± 0.05	This study
SDS	-35.4 ± 0.2	+1.27 ± 0.01	This study
Merck	-39.0 ± 0.1	-	This study
unknown	-39.78 ± 0.08	-	This study
unknown	-	+1.3 ± 0.2	This study
unknown	-	+2.1 ± 0.3	This study
unknown	-31.5 ± 0.3	+2.13 ± 0.03	Jendrzejewski et al. (2001)
unknown	-31.8 ± 0.5	+2.3 ± 0.2	Jendrzejewski et al. (2001)
unknown	-34.19 ± 0.02	+1.555 ± 0.005	Holt et al. (1997)
unknown	-40.4 ± 0.5	-	Holt et al. (1997)
CF	**$\delta^{13}C$ (‰/VPDB)**	**$\delta^{37}Cl$ (‰/SMOC)**	**Reference**
Merck[a]	-48.93 ± 0.08	-	This study
Merck[a]	-52.7 ± 0.1	-	This study
Sigma Aldrich	-	-2.6 ± 0.1	This study
Alfa	-47.96 ± 0.06	-5.9 ± 0.2	This study
Alfa	-47.88 ± 0.08	-5.4 ± 0.3	Breider (2013)
unknown	-43.21 ± 0.04	-1.52 ± 0.01	Holt et al. (1997)
Fluka	-48.7 ± 0.1	-3.0 ± 0.2	Rodríguez-Fernández et al. (2018b), Heckel et al. (2017b)
Acros	-49.76 ± 0.08	-	Rodríguez-Fernández et al. (2018b)
unknown	-51.7 ± 0.4	+0.32 ± 0.08	Jendrzejewski et al. (2001)
Fisher	-53.23 ± 0.09	-	Rodríguez-Fernández et al. (2018b)
Sigma Aldrich	-63.6 ± 0.1	-	Breider (2013)
TCE	**$\delta^{13}C$ (‰/VPDB)**	**$\delta^{37}Cl$ (‰/SMOC)**	**Reference**
unknown	-25.40 ± 0.03	-	This study
unknown	-27.18 ± 0.01	-1.42 ± 0.10	Holt et al. (1997)
PPG	-27.37 ± 0.09	-2.8 ± 0.1	Shouakar-Stash et al. (2003)
unknown	-27.90 ± 0.08	+2.0 ± 0.1	Jendrzejewski et al. (2001)
StanChem	-29.1 ± 0.1	-3.19 ± 0.07	Shouakar-Stash et al. (2003)
ICI	-31.01 ± 0.09	+2.71 ± 0.08	Shouakar-Stash et al. (2003)
Dow	-31.57 ± 0.01	+3.55 ± 0.05	Shouakar-Stash et al. (2003)
Dow	-31.90 ± 0.05	+4.1 ± 0.3	van Warmerdam et al. (1995)
Sigma Aldrich	-33.49 ± 0.08	+3.8 ± 0.1	Jendrzejewski et al. (2001)
MCB	**$\delta^{13}C$ (‰/VPDB)**	**$\delta^{37}Cl$ (‰/SMOC)**	**Reference**
Sigma Aldrich	-27.09 ± 0.07	-	This study
Sigma Aldrich	-25.6[b]	-	Liang et al. (2011)

[a]Solvent with the same reference number but from different batches. [b]$\delta^{13}C$ (‰) value for MCB was obtained from a microcosm experiment where changes in $\delta^{13}C$ by biodegradation of MCB were measured. The initial $\delta^{13}C$ is not considered to be affected by degradation and, therefore, can be assumed as representative of the commercial MCB. VPDB: Vienna Pee Dee Belemnite, SMOC: Standard Mean Ocean Chloride.

920